

Wavelength Reuse in a Symmetrical Radio Over WDM-PON Based on Polarization Multiplexing and Coherent Detection

Xiang Chen, *Student Member, IEEE*, and Jianping Yao, *Fellow, IEEE, Fellow, OSA*

Abstract—A symmetrical radio over a colorless wavelength-division multiplexing passive optical network with wavelength reuse based on polarization multiplexing and coherent detection incorporating digital phase noise cancellation is proposed and experimentally demonstrated. For the downlink, two optical signals are intensity modulated by two different 16-QAM downstream microwave vector signals that are polarization multiplexed at the optical line terminal (OLT). Then, the two orthogonally polarized optical signals are transmitted to the optical network unit (ONU). At the ONU, one of the two orthogonally polarized optical signals is selected to be reused for the uplink transmission. Then, the reused optical signal is split into two channels by a 3-dB coupler. One portion of the reused optical signal is phase modulated by a 16-QAM upstream microwave vector signal, while the other portion is intensity modulated by another 16-QAM upstream microwave vector signal. Again, the two portions of the optical signals are polarization multiplexed and transmitted back to the OLT. At the OLT, a coherent receiver with a digital signal processing (DSP) unit is used to detect the upstream optical signals. Two DSP algorithms are developed to recover the two 16-QAM upstream microwave vector signals. The transmission of two 2.5-Gb/s 16-QAM downstream microwave vector signals and two 2.5-Gb/s 16-QAM upstream microwave vector signals over a 10.5-km single-mode fiber is experimentally demonstrated. The error vector magnitudes for both the down and upstream transmissions are measured to be 7.3% and 8.65%, which are good enough to achieve error-free transmission with forward error correction.

Index Terms—Digital phase noise cancellation, digital signal processing (DSP), laser phase noise, optical coherent detection, polarization multiplexing, symmetrical radio over fiber, wavelength division multiplexing (WDM) passive optical networks (PONs), wavelength reuse.

I. INTRODUCTION

WITH the increasing demand for high-data-rate transmission for broadband wireless access, the provision of wireless services over wavelength division multiplexing (WDM) passive optical networks (PONs) has been a topic of research interest recently. In a radio over WDM-PON, to ease the system installation and maintenance, colorless optical network units (ONUs) are essential. Numerous methods for colorless

operation have been proposed in recent years, including spectrum slicing of a broadband light source that covers a spectral range of all the transmission wavelengths [1], the use of tunable laser sources (TLSs) with a tunable wavelength over a spectral range of transmission [2], and the reuse of the downstream wavelengths [3]–[14]. For the schemes using a broadband light source that covers a spectral range of transmission [1], the modulation bandwidth is usually very narrow due to the poor quality of the spectrum-sliced broadband light source. In addition, such schemes suffer from slicing losses. The use of TLSs at an ONU [2] can solve the two problems. However, it is not a good solution for low-cost implementation because of the very high cost of TLSs. In addition, prior information is required for wavelength tuning at the ONU, which makes the end-to-end control complicated. To reduce the cost and relax the requirements for wavelength management at the ONU side, several schemes have been proposed based on wavelength reuse of a downstream optical signal for upstream transmission, including injection locking of a Fabry–Pérot laser diode (LD) [3]–[6], and the utilization of gain-saturation of a semiconductor optical amplifier (SOA) [7] or a reflective SOA (RSOA) [8]–[10]. However, these schemes require a low modulation depth of the downstream optical signal to reduce the crosstalk to the upstream signal, which limits the transmission performance of the downlink. In addition, the analog bandwidth of an SOA or RSOA is very limited (typically around 1 GHz). To overcome this limitation, two radio over fiber (RoF) systems have been proposed based on the reuse of a phase-modulated downstream optical signal for upstream transmission using a polarization modulator [11]–[13]. However, since two orthogonally polarized light waves, which are phase modulated by a radio signal, are utilized for the purpose of wavelength reuse, polarization multiplexing cannot be employed, which may decrease the spectral efficiency. To solve this problem, recently we have proposed a RoF system with wavelength reuse based on polarization multiplexing and coherent detection [14]. In [14], the polarization multiplexing can be employed, but the system is not symmetrical, since the polarization multiplexing can be only applied for the downlink but not for the uplink, which results in that the data rate for the downlink is twice of that for the uplink.

In this paper, a symmetrical radio over a colorless WDM-PON with wavelength reuse based on polarization multiplexing and coherent detection incorporating digital phase noise cancellation (PNC) is proposed and demonstrated. In the optical line terminal (OLT), polarization multiplexing is employed to double the spectral efficiency and the data rate. In addition,

Manuscript received July 26, 2015; revised October 29, 2015; accepted November 21, 2015. Date of publication November 23, 2015; date of current version February 10, 2016. This work was supported by the Natural Sciences and Engineering Research Council of Canada.

The authors are with the Microwave Photonics Research Laboratory, School of Electrical Engineering and Computer Science, University of Ottawa, Ottawa, ON K1N 6N5, Canada (e-mail: jpyao@eecs.uOttawa.ca).

Color versions of one or more of the figures in this paper are available online at <http://ieeexplore.ieee.org>.

Digital Object Identifier 10.1109/JLT.2015.2503327

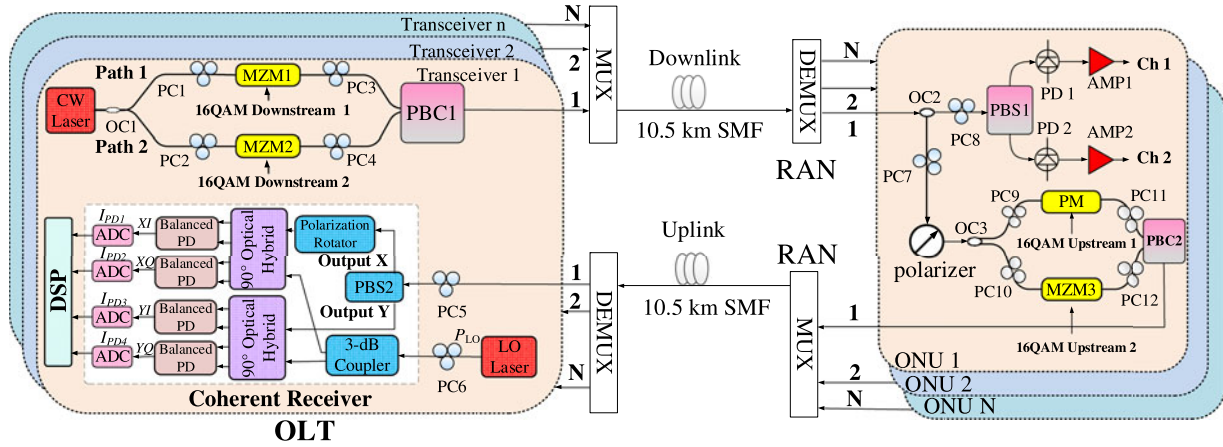


Fig. 1. Schematic diagram of the proposed symmetrical radio over WDM-PON with wavelength reuse based on polarization multiplexing and coherent detection. ADC: analog-to-digital converter, AMP: amplifier, PC: polarization controller, CW laser: continuous-wave laser, Balanced PD: balanced photodetector, PBS: polarization beam splitter, PBC: polarization beam combiner, OC: optical coupler, PM: phase modulator, MZM: Mach-Zehnder modulator, SMF: single-mode fiber, DSP: digital signal processing, OLT: optical line terminal, ONU: optical network unit, LO laser: local oscillator laser, MUX: multiplexer, DEMUX: de-multiplexer.

coherent detection is used for the uplink, to improve the receiver sensitivity and also to compensate for the degraded data transmission performance due to the utilization of a wavelength-reused downstream optical signal. Two digital signal processing (DSP) algorithms for the recovery of two 16-QAM upstream microwave vector signals from the upstream signals, which contain the downstream signals and the phase noises from the transmitter laser source and the local oscillator (LO) laser source, are proposed. In the ONUs, no wavelength selective components are used, making the ONUs colorless. In addition, polarization multiplexing is also employed. Therefore, a symmetrical radio over WDM-PON is implemented. The proposed scheme is experimentally demonstrated. The transmission of two 2.5-Gb/s 16-QAM downstream microwave vector signals and two 2.5-Gb/s 16-QAM upstream microwave vector signals over a 10.5-km single-mode fiber (SMF) is experimentally demonstrated. The error vector magnitudes (EVMs) for the recovered 16-QAM downstream microwave vector signals and the recovered 16-QAM upstream microwave vector signals can reach 7.3% and 8.65%, respectively, which are good enough to achieve error-free transmission with forward error correction (FEC).

II. PRINCIPLE OF OPERATION

The schematic of the proposed symmetrical radio over colorless WDM-PON based on polarization multiplexing and coherent detection incorporating digital PNC is shown in Fig. 1. At a transceiver in the OLT, a continuous-wave (CW) light wave from a LD is equally divided into two channels by a 3-dB coupler (OC1) and sent to two Mach-Zehnder modulators (MZM1 and MZM2) via two polarization controllers (PC1 and PC2). In each path, the CW light wave is intensity-modulated by a 16-QAM microwave vector signal. Both the MZMs are biased at the quadrature point. The two intensity-modulated optical signals are sent via two PCs (PC3 and PC4) and polarization

multiplexed at a polarization beam combiner (PBC1) and sent to a wavelength division multiplexer (MUX). At the MUX, all the optical intensity-modulated signals with different center wavelengths from different transmitters are multiplexed and transmitted to a remote access node (RAN) over an SMF. At the RAN, all the optical intensity-modulated signals are wavelength de-multiplexed via a wavelength division de-multiplexer (DEMUX) and then distributed to the corresponding ONUs. At each ONU, the intensity-modulated light wave is equally divided into two channels by another 3-dB coupler (OC2). The light wave at the upper channel is then polarization de-multiplexed at a polarization beam splitter (PBS1) and detected by two photodetectors (PDs). While the optical signals at the lower channel is sent to a polarizer which is used to select one of the two orthogonally polarized intensity-modulated optical signals. Then the selected intensity-modulated optical signal is split into two portions by a third 3-dB coupler (OC3). One portion is phase-modulated by a 16-QAM upstream microwave vector signal via a phase modulator (PM), while the other portion is intensity-modulated by another 16-QAM upstream microwave vector signal via the third MZM. The two optical signals are polarization multiplexed again at PBC2 and sent to the RAN, where all optical signals from all ONUs are wavelength multiplexed and transmitted over another SMF to the OLT where a DEMUX is used to deliver a different optical wavelength to its corresponding receiver. At each receiver, a polarization- and phase-diversity coherent optical receiver is used to detect the two orthogonally polarized optical upstream signals which are polarization de-multiplexed through a PC (PC5) and the second PBS (PBS2). Four sampled signals (I_{PD1} , I_{PD2} , I_{PD3} and I_{PD4}) at the output of the coherent receiver are sent to a DSP unit which is used to cancel the phase noise and recover the two 16-QAM upstream microwave vector signals.

Mathematically, the two orthogonally polarized intensity-modulated optical signals at the output of PBC1 in the

transmitter can be expressed as

$$\begin{bmatrix} E_{d1}(t) \\ E_{d2}(t) \end{bmatrix} = \sqrt{P_s} \begin{bmatrix} \sqrt{L_{d1}} \cos\left(\frac{\pi S_{RFd1-16QAM}(t)}{2V_{\pi IM1}} + \frac{\pi}{4}\right) e^{j(\omega_c t + \varphi_{c1}(t))} \\ \sqrt{L_{d2}} \cos\left(\frac{\pi S_{RFd2-16QAM}(t)}{2V_{\pi IM2}} + \frac{\pi}{4}\right) e^{j(\omega_c t + \varphi_{c2}(t))} \end{bmatrix} \quad (1)$$

where P_s is the optical output power of the light wave from the transmitter laser source, ω_c is the angular frequency of the optical carrier, $S_{RFd1-16QAM}(t)$ and $S_{RFd2-16QAM}(t)$ are the input microwave vector signals for MZM1 and MZM2, $V_{\pi IM1}$ and $V_{\pi IM2}$ are the half-wave voltages of MZM1 and MZM2, and $\varphi_{c1}(t)$ and $\varphi_{c2}(t)$ are the phase terms of the transmitter laser source for Path 1 and Path 2. Note, $\varphi_{c1}(t)$ and $\varphi_{c2}(t)$ are different, since the optical signals from the transmitter laser source are split and transmitted through two different paths. L_{d1} and L_{d2} are the link losses between OC1 and PBS1 for Path 1 and Path 2, respectively.

Then, the two intensity-modulated light waves from the two paths are polarization multiplexed at PBC1 and multiplexed with other wavelengths. After transmission over an SMF, the optical signals are wavelength de-multiplexed at the RAN and sent to the corresponding ONUs.

At an ONU, the two received orthogonally polarized intensity-modulated light waves are divided into two parts by a 3-dB optical coupler. The upper part is polarization de-multiplexed at a polarization beam splitter (PBS1) and detected by two PDs. The photocurrents after the two PDs can be expressed as

$$\begin{aligned} I_{d1} &= R_1 \cdot \left[\sqrt{L_f} E_{d1}(t) / \sqrt{2} \right] \cdot \left[\sqrt{L_f} E_{d1}^*(t) / \sqrt{2} \right] / 2 \\ &= R_1 P_s L_{d1} L_f \left(1 - \sin\left(\frac{\pi S_{RFd1-16QAM}(t)}{V_{\pi IM1}}\right) \right) / 8 \\ &\approx R_1 P_s L_{d1} L_f \left(1 - \frac{\pi S_{RFd1-16QAM}(t)}{V_{\pi IM1}} \right) / 8 \quad (2) \end{aligned}$$

$$\begin{aligned} I_{d2} &= R_2 \cdot \left[\sqrt{L_f} E_{d2}(t) / \sqrt{2} \right] \cdot \left[\sqrt{L_f} E_{d2}^*(t) / \sqrt{2} \right] / 2 \\ &\approx R_2 P_s L_{d2} L_f \left(1 - \frac{\pi S_{RFd2-16QAM}(t)}{V_{\pi IM2}} \right) / 8 \quad (3) \end{aligned}$$

where R_1 and R_2 are the responsivities for PD1 and PD2, respectively. L_f is the link loss caused by the SMF.

The lower part is sent to a polarizer which is used to select one of the two orthogonally polarized intensity-modulated optical signals (Here, we suppose that the optical signal for Path 1 is selected.) and then the selected signal is split by a 3-dB optical coupler. One portion is phase modulated by a 16-QAM upstream microwave vector signal and the other is intensity-modulated by another 16-QAM upstream microwave vector signal. The two optical signals are then polarization multiplexed at PBC2. The optical fields of the two orthogonally polarized optical signals

at the output of PBC2 are given by

$$\begin{bmatrix} E_{up1}(t) \\ E_{up2}(t) \end{bmatrix} = \begin{bmatrix} A \\ B \end{bmatrix} \quad (4)$$

with

$$\begin{aligned} A &= \frac{\sqrt{P_s L_{d1} L_{up1} L_f}}{2} \cos\left[\frac{\pi S_{RFd1-16QAM}(t)}{2V_{\pi IM1}} + \frac{\pi}{4}\right] \\ &\quad \times \exp\{j[\omega_c t + \varphi_{c3}(t) + \pi S_{RFup1-16QAM}(t) / V_{\pi PM}]\} \\ B &= \frac{\sqrt{P_s L_{d1} L_{up2} L_f}}{2} \cos\left[\frac{\pi S_{RFd1-16QAM}(t)}{2V_{\pi IM1}} + \frac{\pi}{4}\right] \\ &\quad \times \cos\left[\frac{\pi S_{RFup2-16QAM}(t)}{2V_{\pi IM3}} + \frac{\pi}{4}\right] \exp\{j[\omega_c t + \varphi_{c4}(t)]\} \end{aligned}$$

where L_f is the link loss caused by the SMF, L_{up1} and L_{up2} are the link losses between OC3 and PBC2 for the upper channel and the lower channel. $\varphi_{c3}(t)$ and $\varphi_{c4}(t)$ are the phase terms of the transmitter laser source for the upper and the lower channels. Note again $\varphi_{c3}(t)$ and $\varphi_{c4}(t)$ are different. $V_{\pi IM3}$ and $V_{\pi PM}$ are the half-wave voltages of MZM3 and the PM, respectively.

The wavelength-reused two orthogonally polarized light waves carrying the upstream data are transmitted to the RAN and sent to the OLT over another SMF.

At the OLT, the two orthogonally polarized light waves are polarization de-multiplexed by PBS2. The optical fields at the outputs of PBS2 for Output X and Output Y are given by

$$E_x(t) = \sqrt{L_f} E_{up1}(t) \quad (5)$$

$$E_y(t) = \sqrt{L_f} E_{up2}(t). \quad (6)$$

On the other hand, the optical field at the output of the LO laser source can be written as

$$E_{LO}(t) = \sqrt{2P_{LO}} e^{j[\omega_{LO} t + \varphi_{LO}(t)]} \quad (7)$$

where P_{LO} is the optical power of the light wave from the LO laser source, $\varphi_{LO}(t)$ is the phase term, and ω_{LO} is the angular frequency.

Through tuning PC6, with the help of the polarization rotator in Fig. 1, the light wave from the LO laser source is co-polarized with the other optical signals at the inputs of the two 90° optical hybrids. At the outputs of the two 90° optical hybrids, eight optical fields are obtained, given by

$$\begin{aligned} &\begin{pmatrix} E_1(t) & E_2(t) & E_3(t) & E_4(t) \\ E_5(t) & E_6(t) & E_7(t) & E_8(t) \end{pmatrix} \\ &= \sqrt{L_h} \begin{pmatrix} E_x(t) & E_{LO}(t) e^{j\varphi_x} / \sqrt{2} \\ E_y(t) & E_{LO}(t) e^{j\varphi_y} / \sqrt{2} \end{pmatrix} \\ &\quad \cdot \begin{pmatrix} 1 & 1 & 1 & 1 \\ 1 & e^{j\pi} & e^{j\pi/2} & e^{-j\pi/2} \end{pmatrix} \quad (8) \end{aligned}$$

where φ_x and φ_y are the phase terms arising from the polarization mismatch between the upstream optical signal and the light wave from LO laser source. By applying (E_1, E_2) , (E_3, E_4) , (E_5, E_6) , (E_7, E_8) to four identical balanced PDs which are

terminated with 50-Ω resistors, four output photocurrents are obtained, which are given by

$$I_{PD1} = RL_h L_f \sqrt{P_s P_{LO} L_{d1} L_{up1}} \cos [\pi S_{RFd1-16QAM}(t) / 2V_{\pi IM1} + \pi/4] \times \cos [\Delta\omega t + \varphi_{c3}(t) + \pi S_{RFup1-16QAM}(t) / V_{\pi PM} - \varphi_x] \quad (9)$$

$$I_{PD2} = RL_h L_f \sqrt{P_s P_{LO} L_{d1} L_{up1}} \cos [\pi S_{RFd1-16QAM}(t) / 2V_{\pi IM1} + \pi/4] \times \sin [\Delta\omega t + \varphi_{c3}(t) + \pi S_{RFup1-16QAM}(t) / V_{\pi PM} - \varphi_x] \quad (10)$$

$$I_{PD3} = RL_h L_f \sqrt{P_s P_{LO} L_{d1} L_{up2}} \cos [\pi S_{RFd1-16QAM}(t) / 2V_{\pi IM1} + \pi/4] \times \cos [\pi S_{RFup2-16QAM}(t) / 2V_{\pi IM3} + \pi/4] \cos [\Delta\omega t + \varphi_{c4}(t) - \varphi_y] \quad (11)$$

$$I_{PD4} = RL_h L_f \sqrt{P_s P_{LO} L_{d1} L_{up2}} \cos [\pi S_{RFd1-16QAM}(t) / 2V_{\pi IM1} + \pi/4] \times \cos [\pi S_{RFup2-16QAM}(t) / 2V_{\pi IM3} + \pi/4] \sin [\Delta\omega t + \varphi_{c4}(t) - \varphi_y] \quad (12)$$

where R is the responsivity for the balanced PDs.

Through the DSP, we can have

$$I_1 = \tan^{-1} \left[\frac{(I_{PD2} \times I_{PD3} - I_{PD1} \times I_{PD4})}{(I_{PD1} \times I_{PD3} + I_{PD2} \times I_{PD4})} \right] = \tan^{-1} \left\{ \frac{\sin [\pi S_{RFup1-16QAM}(t) / V_{\pi PM} + \varphi(t)]}{\cos [\pi S_{RFup1-16QAM}(t) / V_{\pi PM} + \varphi(t)]} \right\} = \pi S_{RFup1-16QAM}(t) / V_{\pi PM} + \varphi(t) \quad (13)$$

with

$$\varphi(t) = \varphi_{c3}(t) - \varphi_{c4}(t) - \varphi_x + \varphi_y.$$

In (13), the maximum frequency of $\varphi(t)$ is determined by the linewidth of the transmitter laser source. If the spectrum of $S_{RFup1-16QAM}(t)$ does not overlap with that of $\varphi(t)$, $S_{RFup1-16QAM}(t)$ can be selected via a digital bandpass filter, which is free from the phase noise.

Also, through DSP we can have,

$$I_2 = (I_{PD3}^2 + I_{PD4}^2) / (I_{PD1}^2 + I_{PD2}^2) = L_{up2} / L_{up1} \times \{ \cos [\pi S_{RFup2-16QAM}(t) / 2V_{\pi IM3} + \pi/4] \}^2 = L_{up2} / L_{up1} \times \{ 1 - \sin [\pi S_{RFup2-16QAM}(t) / V_{\pi IM3}] \} / 2 \approx L_{up2} / L_{up1} \times [1 - \pi S_{RFup2-16QAM}(t) / V_{\pi IM3}] / 2. \quad (14)$$

As can be seen, a recovery of the signal, $S_{RFup2-16QAM}(t)$, free from the phase noise, is realized.

III. EXPERIMENT

An experiment based on the setup shown in Fig. 2 is conducted. A CW light wave from a TLS (Agilent N7714A) operating at 1550.445 nm with a linewidth of 100 kHz and an optical power of 16.0 dBm is split into two paths by OC1. In each channel, the CW light is intensity-modulated by a 16-QAM downstream microwave vector signal via its corresponding MZM (MZM1 and MZM2). Note that PC1 and PC2 are used to minimize the polarization dependent loss at MZM1 (JDSU) and MZM2 (JDSU), and PC3 and PC4 are used to make the polarization directions of the two optical signals align with the two principal axes of PBC1, thus the two light waves are polarization multiplexed and transmitted to the ONU over a 10.5 km SMF. The bandwidth of the MZMs at the OLT is 10 GHz and the half-wave voltage is around 5.5 V. At the ONU, the two orthogonally polarized intensity-modulated signals are equally divided by OC2. The light wave at the upper channel is then polarization de-multiplexed at a polarization beam splitter (PBS1) and detected by two PDs (New Focus, Model: 1414-50) with a bandwidth of 20 GHz and a responsivity of 0.6 A/W. While the optical signal at the lower channel is sent to a polarizer via PC7 (Here, PC7 and PC8 can be replaced by a dynamic polarization controller in a practical system [15]), which is used to select one of the two orthogonally polarized intensity-modulated optical signals. The selected intensity-modulated optical signal is split again by OC3 for wavelength reuse. One portion is phase modulated by a 16-QAM upstream microwave vector signal at the PM (JDSU) with a bandwidth of 20 GHz and a half-wave voltage of 5 V, while the other portion is intensity-modulated by another 16-QAM upstream microwave vector signal at MZM3 (JDSU) with a bandwidth of 10 GHz and a half-wave voltage of 5.5 V. All the downstream and upstream 16-QAM microwave vector signals are generated by an arbitrary waveform generator (Tektronix AWG7102). The symbol rates and the center frequencies for the 16-QAM microwave vector signals are all 2.5 Gb/s and 2.5 GHz. Again, the two portions of optical signals are polarization multiplexed at PBC2 and transmitted to the OLT over another 10.5 km SMF. At the OLT, a coherent receiver (Discovery Semiconductors DP-QPSK 40/100 Gb/s Coherent Receiver Lab Buddy) is used to detect the upstream optical signals. Through tuning PC5 (Here, PC5 can be replaced by a dynamic PC in a practical system [15]), the two polarization multiplexed light waves can be polarization de-multiplexed by PBS2, which is inside the coherent receiver. In the experiment, at the output X of PBS2, the optical signal for Channel A is obtained, while the optical signal for Channel B is obtained at the other output of PBS2. On the other hand, a second TLS (Yokogawa AQ2201) which has a center wavelength of 1550.476 nm, a linewidth of 1 MHz and an output optical power of 9 dBm is used as the LO laser source. The light wave from the LO laser source is sent to the LO port of the coherent receiver through PC6. Through tuning PC5 and PC6, with the help of the polarization rotator in Fig. 2, the light wave from the LO laser source is co-polarized with the other upstream optical signals at the inputs of the two 90° optical hybrids. After coherent detection, at the output of the coherent receiver, a Digital Storage Oscilloscope (Agilent

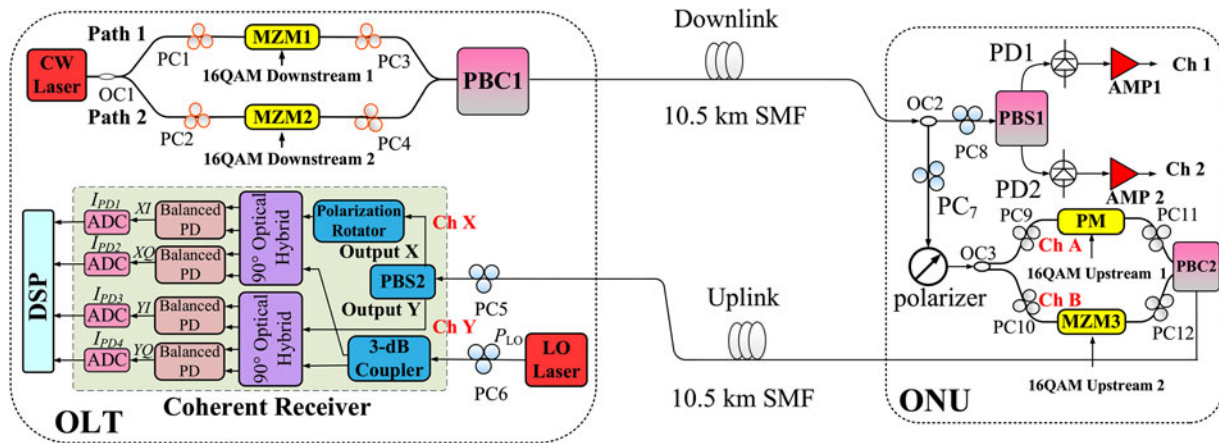


Fig. 2. Experimental setup of the proposed symmetrical radio over WDM-PON with wavelength reuse based on polarization multiplexing and coherent detection. ADC: analog-to-digital converter, PC: polarization controller, CW laser: continuous-wave laser, Balanced PD: balanced photodetector, PBS: polarization beam splitter, PBC: polarization beam combiner, OC: optical coupler, PM: phase modulator, MZM: Mach-Zehnder modulator, SMF: single mode fiber, DSP: digital signal processing, OLT: optical line terminal, ONU: optical network unit, LO laser: local oscillator laser.

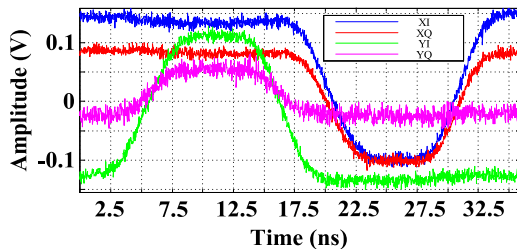


Fig. 3. Temporal waveforms at the outputs of the coherent receiver (XI, XQ, YI, YQ).

DSO-X 93204A) is employed to perform the analog-to-digital conversion at a sampling rate of 40 GSa/s. The sampled signals (I_{PD1} , I_{PD2} , I_{PD3} and I_{PD4}) are processed off-line in a computer with the proposed DSP algorithms developed to recover the two 16-QAM upstream vector signals, which is discussed in Section II.

Note that the time delays of Channel A and Channel B should be equal. To evaluate the relative time delay between Channel A and Channel B, a CW light wave which is intensity modulated by an electrical pulse is sent through a 1×2 coupler into Channel A and Channel B. Then, the light waves from the two channels are polarization multiplexed at the PBC, sent to a coherent receiver and polarization de-multiplexed at the PBS inside the coherent receiver. A real-time oscilloscope (Agilent DSO-X 93204A) is employed to monitor the four signals at the outputs of the coherent receiver. Fig. 3 shows the temporal waveforms of the four signals. As can be seen, the relative time delays between XI and XQ, YI and YQ are small and can be ignored. However, the relative time delay between Channel A and Channel B is about 14.625 ns ($585/40e9$ s) which is large and cannot be ignored. In order to recover the two 16-QAM upstream microwave vector signals (signal 1 and signal 2), the relative time delay between Channel A and Channel B is controlled precisely identical by the DSP unit. In addition, the length differences of the cables at

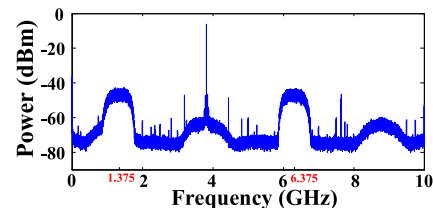


Fig. 4. Spectra of the signals at the second output port of the coherent receiver (I_{PD2}).

the outputs of the coherent receiver between the four paths are controlled within 1 mm.

Fig. 4 shows the spectrum at the second output of the coherent receiver (I_{PD2}), which contains 16-QAM upstream microwave vector signal 1 and 16-QAM downstream microwave vector signal 1. Due to the frequency difference between the transmitter laser source and the LO laser source, the center frequencies of the transmitted microwave vector signals are changed at the outputs of the coherent receiver which can be seen in Fig. 4. The detected microwave vector signals (the signals with the center frequencies of 1.375 and 6.375 GHz) at the second output of the coherent receiver are the mixing products of the 2.5-GHz transmitted microwave vector signals and the 3.875-GHz electrical carrier whose frequency is just the frequency difference between the two laser sources. In addition, the spectra of 16-QAM upstream microwave vector signal 1 and 16-QAM downstream microwave vector signal 1 are completely overlapped. Figs. 5 and 6 show the spectra of the recovered 16-QAM upstream microwave vector signal 1 and 16-QAM upstream microwave vector signal 2 at the output of the DSP unit. The center frequencies of the detected signals at the outputs of the coherent receiver are recovered to their original center frequencies (2.5 GHz) after the processing, which demonstrate that the DSP algorithm cancels the frequency difference successfully.

To evaluate the transmission performance of the system, first we measure the EVMs for the recovered two 16-QAM upstream

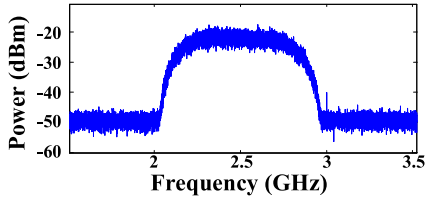


Fig. 5. Spectrum of the recovered 16-QAM upstream microwave vector signal 1 at the output of the DSP unit.

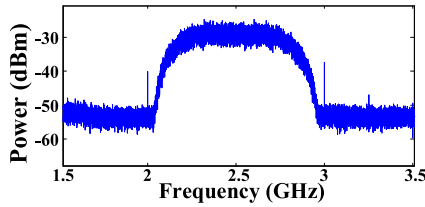


Fig. 6. Spectrum of the recovered 16-QAM upstream microwave vector signal 2 at the output of the DSP unit.

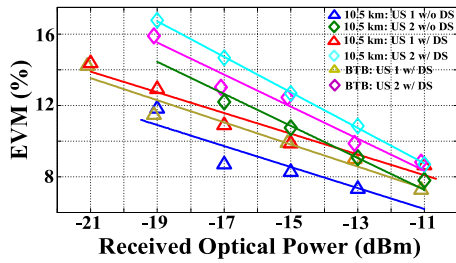


Fig. 7. EVM measurements at different received optical power levels for the 16-QAM upstream microwave vector signal 1 and the 16-QAM upstream microwave vector signal 2. US 1: upstream signal 1, US 2: upstream signal 2, DS: downstream signal, BTB: back to back.

vector signals versus the received optical power which is shown in Fig. 6 (Here, the received optical power refers to the optical power at the output of PC5). Three different situations are considered: first, the reused optical light is a pure optical carrier (fiber length: 10.5 km); second, the reused optical light is intensity-modulated by a downstream microwave vector signal (fiber length: 0 km), and third, the reused optical light is intensity-modulated by a downstream microwave vector signal (fiber length: 10.5 km). As can be seen in Fig. 7, the power penalty caused by the wavelength reuse is about 3.4 dB for upstream signal 1 and it is around 2 dB for upstream signal 2, while the power penalty caused by the fiber transmission is around 1 dB. For the third situation, the constellations of the two recovered 16-QAM microwave vector signals are shown in Fig. 8. It can be seen that when the received optical power (Here, the received optical power refers to the optical power at the output of PC5) is -11 dBm, the constellations are quite clear for both upstream signals. The corresponding estimated BERs as a function of the received optical power are also calculated, which are shown in Fig. 9. Here, the noise after the digital PNC module is assumed as a stationary random process with Gaussian statistics. Thus, we can calculate the BERs of M -ary QAM

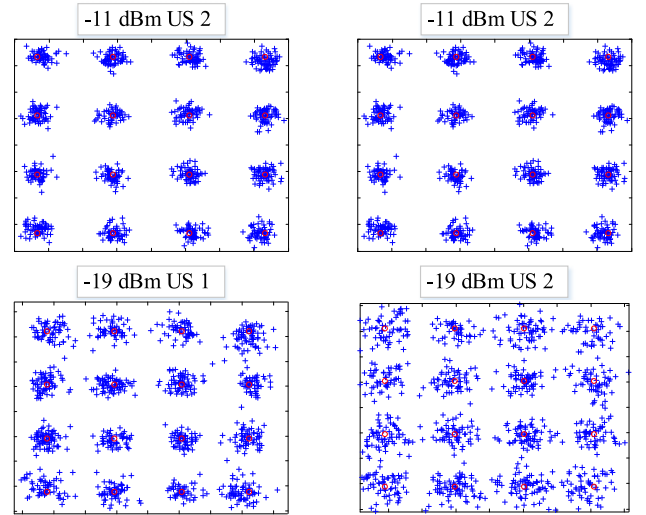


Fig. 8. Constellations diagrams of the two recovered 16-QAM upstream microwave vector signals at the output of the DSP unit. US 1: upstream signal 1, US 2: upstream signal 2.

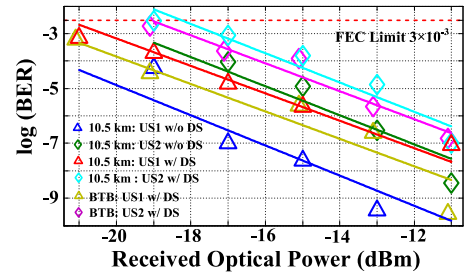


Fig. 9. Estimated BERs at different received optical power levels for the 16-QAM upstream microwave vector signal 1 and the 16-QAM upstream microwave vector signal 2. US 1: upstream signal 1, US 2: upstream signal 2, DS: downstream signal, BTB: back to back.

from the EVMs based on the relationship given by

$$\bar{P}_{M-QAM} = \frac{2}{\log_2 M} \left(1 - \frac{1}{\sqrt{M}} \right) \times \operatorname{erfc} \left(\sqrt{\frac{3}{2(M-1)} \times SNR} \right) \quad (15)$$

with

$$SNR = 1/EVM^2 \quad (16)$$

where $\operatorname{erfc}()$ denotes the complementary error function and SNR is signal-to-noise ratio [16]–[19].

When the received optical power is only -19 dBm, the BERs of the two recovered upstream signals are still less than 3×10^{-3} . By using the FEC technique, error-free transmission can be achieved [20], [21] (The FEC technique can be applied to improve a raw BER of up to 3×10^{-3} to an effective BER of 1×10^{-15} , at the expense of a 6.7% overhead [21]).

As can be seen in Fig. 9, the transmission performance (BERs) of 16-QAM upstream microwave vector signal 1 is better than that of 16-QAM upstream microwave vector signal 2. The reason is that the link loss of Channel A is less than that of Channel B.

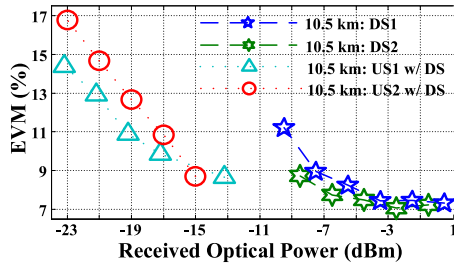


Fig. 10. EVMs at different received optical power levels for the two 16-QAM downstream signals and the two 16-QAM upstream signals. US 1: upstream signal 1, US 2: upstream signal 2, DS: downstream signal, DS 1: downstream signal 1, DS 2: downstream signal 2.

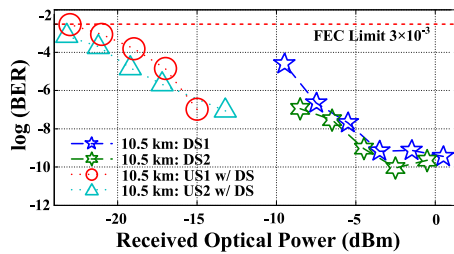


Fig. 11. Estimated BERs at different received optical power levels for the two 16-QAM downstream signals and the two 16-QAM upstream signals. US 1: upstream signal 1, US 2: upstream signal 2, DS: downstream signal, DS 1: downstream signal 1, DS 2: downstream signal 2.

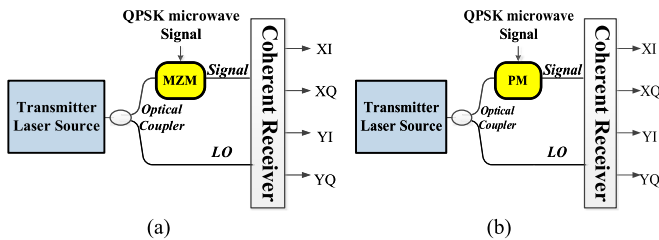


Fig. 12. Schematic diagrams of (a) an IM/CD link and (b) a PM/CD link without digital PNC unit.

Second, we measure the EVMs versus the received optical power for the two 16-QAM downstream signals, which is shown in Fig. 10. In Fig. 10, the received optical power for downstream signal 1 and downstream signal 2 refer to the optical power at the inputs of the corresponding PDs. While the received optical power for upstream signal 1 and upstream signal 2 refers to the received optical power after the PC5 from Channel A and Channel B, respectively. It can be seen in Fig. 10, since coherent detection is used for the upstream signals, the receiver sensitivity for the uplink is much better than that for the downlink. Fig. 11 shows the corresponding estimated BERs as a function of the received optical power.

To verify the effectiveness of the proposed PNC technique which has been discussed in Section II, we also measure the constellations of the detected signals for an intensity-modulation coherent detection (IM/CD) link and a phase-modulation coherent detection (PM/CD) link without a digital PNC module. The experiment setups are shown in Fig. 12(a) and (b). Here, the microwave vector signal for both setups is a QPSK signal with

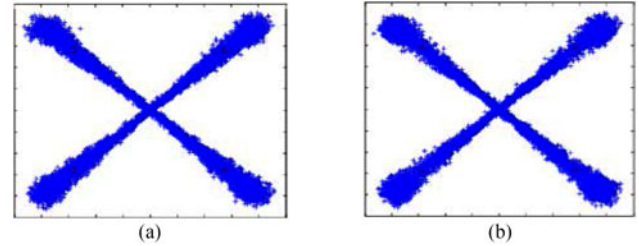


Fig. 13. Constellations of the detected QPSK microwave vector signals. (a) The IM/CD link without digital PNC unit, (b) the PM/CD link without digital PNC unit.

a center frequency of 2.5 GHz and a symbol rate of 625 MSymbol/s. The linewidth of the laser source is 100 KHz. Since the optical signals for the signal port and LO port of the coherent receiver come from the same laser source, the frequency difference between the transmitter laser source and LO laser source does not exist. So the detected signals at the outputs of the coherent receiver are affected only by the phase noise. Fig. 13(a) and (b) shows the constellations of the output signals at the XI ports of the coherent receivers in Fig. 13(a) and (b). As can be seen, the quality of the recovered QPSK microwave vector signals is very poor. Therefore, the clear constellations in Fig. 8 demonstrate the effectiveness of the proposed PNC technique.

IV. DISCUSSIONS

In order to have a better understanding the characteristics of the proposed scheme, a comparison (complexity vs. performance) is made between the proposed scheme and other schemes for colorless operation, which is shown in Table I. As can be seen, although the coherent receiver is expensive, it is installed in the OLTs, so it will be shared by multiple ONUs, which may reduce the cost of the entire system. In addition, coherent detection can provide very high receiver sensitivity which may reduce the number of the EDFAs required in the system. So the proposed scheme is a viable solution for the implementation of symmetrical radio over WDM-PON system.

V. CONCLUSION

A symmetrical radio over colorless WDM-PON based on polarization multiplexing and coherent detection incorporating digital PNC was proposed and experimentally demonstrated. For upstream transmission, wavelength reuse was employed, thus colorless WDM-PON was enabled. The wavelength reuse was achieved with the help of coherent detection, to eliminate the impact from the downstream signals. In addition, the symmetry of the network was achieved by using polarization multiplexing for both the downstream and upstream signals, thus the spectral efficiency was also increased. Furthermore, coherent detection with DSP for upstream transmission also increased the receiver sensitivity. The proposed symmetrical radio over colorless WDM-PON was evaluated experimentally. With the proposed DSP algorithms, two 16-QAM upstream signals modulated on a reused wavelength carrying one of the two downstream signals and with phase noises from the transmitter laser source and the LO laser source were successfully recovered.

TABLE I
COMPARISON OF DIFFERENT SCHEMES FOR COLORLESS ONU S

Scheme	Bit rate	Advantages	Disadvantages	Complexity
Spectrum slicing LED [1]	< 155 Mb/s	Cheap, no seed needed	Poor scalability and reach	Low
Injection locked FP-LD [3]	> 2.5 Gb/s	Inexpensive, relatively high bit rate	Non-standard FP-LD may be needed	Medium
RSOA with re-modulation [8]–[10]	> 2.5 Gb/s	Relatively high bit rate, no seed source	Downstream modulation index is limited	Medium
Tunable laser [2]	> 10 Gb/s	No seed needed, high bit rate	Too expensive, wavelength assignment algorithm is needed	Very complex
Our system	> 10 Gb/s	High receiver sensitivity, no seed needed, high bit rate	Expensive coherent receiver is needed in the OLT	Medium

In the experiment, the transmission of two 2.5-Gb/s 16-QAM downstream microwave signals and two 2.5-Gb/s 16-QAM upstream microwave signals over a 10.5-km SMF was experimentally demonstrated.

REFERENCES

- [1] D. K. Jung, S. K. Shin, C. -H. Lee, and Y. C. Chung, "Wavelength-division-multiplexed passive optical network based on spectrum-slicing techniques," *IEEE Photon. Technol. Lett.*, vol. 10, no. 9, pp. 1334–1336, Sep. 1998.
- [2] J. Zhang and A. Ansari, "Design of WDM PON with tunable lasers: the upstream scenario," *J. Lightw. Technol.*, vol. 28, no. 2, pp. 228–236, Jan. 2010.
- [3] W. Cui, T. Shao, and J. P. Yao, "Wavelength reuse in a UWB over WDM-PON based on injection locking of a Fabry-Pérot laser diode and polarization multiplexing," *J. Lightw. Technol.*, vol. 32, no. 2, pp. 220–227, Jan. 2014.
- [4] Y.-C. Su, Y.-C. Chi, H.-Y. Chen, and G.-R. Lin, "All colorless FPLD-based bidirectional full-duplex DWDM-PON," *J. Lightw. Technol.*, vol. 33, no. 4, pp. 832–842, Feb. 15, 2015.
- [5] Y.-C. Chi, Y.-C. Li, H.-Y. Wang, P.-C. Peng, H.-H. Lu, and G.-R. Lin, "Optical 16-QAM-52-OFDM transmission at 4 Gbit/s by directly modulating a coherently injection-locked colorless laser diode," *Opt. Exp.*, vol. 20, no. 18, pp. 20071–20077, Aug. 2012.
- [6] F. Xiong, W.-D. Zhong, and H. Kim, "A broadcast-capable WDM-PON based on polarization-sensitive weak-resonant-cavity Fabry-Pérot laser diodes," *J. Lightw. Technol.*, vol. 30, no. 3, pp. 355–361, Feb. 2012.
- [7] H. Takesue and T. Sugie, "Wavelength channel data rewrite using saturated SOA modulator for WDM networks with centralized light sources," *J. Lightw. Technol.*, vol. 21, no. 11, pp. 2546–2556, Nov. 2003.
- [8] W. Lee, M. Y. Park, S. H. Cho, J. Lee, C. Kim, G. Jeong, and B. W. Kim, "Bidirectional WDM-PON based on gain-saturated reflective semiconductor optical amplifiers," *IEEE Photon. Technol. Lett.*, vol. 17, no. 11, pp. 2160–2162, Nov. 2005.
- [9] A. T. Nguyen, K. Lefebvre, and L. A. Rusch, "Multi-service OFDM uplink transmission in full-duplex FTTx systems using RSOA-based WDM-PON architecture," presented at the Optical Fiber Communication Conf., San Francisco, CA, USA, Mar. 9–13, 2014, Paper Tu2C.1.
- [10] K. Lefebvre, A. T. Nguyen, and L. A. Rusch, "Enabling in-band bidirectional OFDM-uplink and OOK-downlink transmission in long-reach RSOA-based WDM-PON systems," *J. Lightw. Technol.*, vol. 32, no. 20, pp. 3854–3860, Oct. 15, 2014.
- [11] T. Shao and J. P. Yao, "Wavelength reuse in a bidirectional UWB over fiber system," *Opt. Exp.*, vol. 21, no. 10, pp. 11921–11927, Apr. 2013.
- [12] J. Zheng, H. Wang, L. Wang, N. Zhu, J. Liu, and S. Wang, "Implementation of wavelength reusing upstream service based on distributed intensity conversion in ultrawideband-over-fiber system," *Opt. Lett.*, vol. 38, no. 7, pp. 1167–1169, Apr. 2013.
- [13] B. Wu, M. Zhu, J. Zhang, J. Wang, M. Xu, F. Yan, S. Jian, and G. K. Chang, "Multi-service RoF links with colorless upstream transmission based on orthogonal phase-correlated modulation," *Opt. Exp.*, vol. 23, no. 14, pp. 18323–18329, Jul. 2015.
- [14] X. Chen and J. P. Yao, "Radio over colorless WDM-PON with wavelength reuse based on polarization multiplexing and coherent detection incorporating digital phase noise cancellation," presented at the Optical Fiber Communication Conf., Los Angeles, CA, USA, Mar. 22–26, 2015, Paper WIF.2.
- [15] X. S. Yao, L. -S. Yan, B. Zhang, A. E. Willner, and J. Jiang, "All-optic scheme for automatic polarization division demultiplexing," *Opt. Exp.*, vol. 15, no. 12, pp. 7407–7414, Jun. 2007.
- [16] D. H. Wolaver, "Measure error rates quickly and accurately," *Electron. Des.*, vol. 43, no. 11, pp. 89–98, May 1995.
- [17] A. Brilliant, *Digital and Analog Fiber Optic Communication for CATV and FTTx Applications*. Bellingham, WA, USA: SPIE, 2008, pp. 653–660.
- [18] V. J. Urlick, J. X. Qiu, and F. Bucholtz, "Wide-band QAM-over-fiber using phase modulation and interferometric demodulation," *IEEE Photon. Technol. Lett.*, vol. 16, no. 10, pp. 2374–2376, Oct. 2004.
- [19] G. P. Agrawal, *Fiber-Optic Communication Systems*, 4th ed. Hoboken, NJ, USA: Wiley, 2010, pp. 151–157.
- [20] G. Hill, *The Cable and Telecommunications Professionals' Reference: Transport Networks*, vol. 3. Burlington, MA, USA: Focal Press, 2008, pp. 203–206.
- [21] R. Schmogrow, D. Hillerkuss, S. Wolf, B. Bäuerle, M. Winter, P. Kleinow, B. Nebendahl, T. Dippon, P. C. Schindler, C. Koos, W. Freude, and J. Leuthold, "512QAM Nyquist sinc-pulse transmission at 54 Gbit/s in an optical bandwidth of 3 GHz," *Opt. Exp.*, vol. 20, no. 6, pp. 6439–6447, Mar. 2012.

Xiang Chen (S'13) received the B.Eng. degree in communications engineering from Donghua University, Shanghai, China, in 2009, and the M.Sc. degree in communications and information engineering from Shanghai University, Shanghai, in 2012. He is currently working toward the Ph.D. degree in electrical and computer engineering at the Microwave Photonics Research Laboratory, School of Electrical Engineering and Computer Science, University of Ottawa, Ottawa, ON, Canada.

His current research interests include coherent radio-over-fiber systems and the dynamic range of analog optical links.

Jianping Yao (M'99–SM'01–F'12) received the Ph.D. degree in electrical engineering from the Université de Toulon, Toulon, France, in December 1997.

He is a Professor and the University Research Chair at the School of Electrical Engineering and Computer Science, University of Ottawa, Ottawa. He joined the School of Electrical and Electronic Engineering, Nanyang Technological University, Singapore, as an Assistant Professor in 1998. In December 2001, he joined the School of Electrical Engineering and Computer Science, University of Ottawa, as an Assistant Professor, where he became an Associate Professor in 2003, and a Full Professor in 2006. He was appointed the University Research Chair in Microwave Photonics in 2007. From July 2007 to June 2010, he was the Director of the Ottawa-Carleton Institute for Electrical and Computer Engineering. He was reappointed as the Director of the Ottawa-Carleton Institute for Electrical and Computer Engineering in 2013. He has published more than 500 papers, including more than 290 papers in peer-reviewed journals and 210 papers in conference proceedings. He was a Guest Editor for the Focus Issue on Microwave Photonics in *Optics Express* in 2013 and a Feature Issue on Microwave Photonics in *Photonics Research* in 2014. He is currently a Topical Editor for *Optics Letters*, and serves on the Editorial Board of the IEEE TRANSACTIONS ON MICROWAVE THEORY AND TECHNIQUES, *Optics Communications*, and *China Science Bulletin*.

Dr. Yao is a Chair of numerous international conferences, symposia, and workshops, including the Vice Technical Program Committee (TPC) Chair of the IEEE Microwave Photonics Conference in 2007, the TPC Cochair of the Asia-Pacific Microwave Photonics Conference in 2009 and 2010, the TPC Chair of the high-speed and broadband wireless technologies subcommittee of the IEEE Radio Wireless Symposium in 2009–2012, the TPC Chair of the microwave photonics subcommittee of the IEEE Photonics Society Annual Meeting in 2009, the TPC Chair of the IEEE Microwave Photonics Conference in 2010, the General Cochair of the IEEE Microwave Photonics Conference in 2011, the TPC Cochair of the IEEE Microwave Photonics Conference in 2014, and the General Cochair of the IEEE Microwave Photonics Conference in 2015. He received the 2005 International Creative Research Award at the University of Ottawa, the 2007 George S. Glinski Award for Excellence in Research, and the OSA Outstanding Reviewer Award in 2012. He is an IEEE MTT-S Distinguished Microwave Lecturer for 2013–2015. He is a registered Professional Engineer of Ontario. He is a Fellow of the Optical Society of America and the Canadian Academy of Engineering.